ACS SENSORS

pubs.acs.org/acssensors Article

A Carbon-Based DNA Framework Nano−Bio Interface for Biosensing with High Sensitivity and a High Signal-to-Noise Ratio

Jing Su,[#] Wenhan Liu,[#] Shixing Chen, Wangping Deng, Yanzhi Dou, Zhihan Zhao, Jianyong Li, Zhenhua Li, Heng Yin, Xianting Ding,* and Shiping Song*

Cite This: https://dx.doi.org/10.1021/acssensors.0c01745 Read Online

ACCESS | Metrics & More | Article Recommendations | Supporting Information

ABSTRACT: Biosensing interface based on screen-printed carbon electrodes (SPCE) has been widely used for electrochemical biosensors in the field of medical diagnostics, food safety, and environmental monitoring. Nevertheless, SPCE always has a rough surface, which is easy to result in the disorder of nucleic acid capture probes, the nonspecific adsorption of signaling probes, the steric hindrance of target binding, and decrease in the signal-to-noise ratio and sensitivity of biosensors. So far, it still remains extremely challenging to develop high-efficiency carbon-based biosensing interfaces, especially for DNA probe-based assembly and functionalization. In this paper, we first used a specific DNA framework, DNA tetrahedron to solve the defects of the carbon interface, improving the biosensing ability of SPCE. With covalent coupling, the DNA tetrahedron could be immobilized on the carbon surface. Biosensing probe sequences extending from the DNA tetrahedron can be changed for different target molecules. We demonstrated that the improved SPCE could be applied for the detection of a variety of bioactive molecules. Typically, we designed gap hybridization, aptamer "sandwich" and aptamer competition reduction strategy for the detection of miRNA-141, thrombin, and ATP, respectively. High signal-to-noise ratio, sensitivity, and specificity were obtained for all of these kinds. Especially, the DNA tetrahedron-modified SPCE can work well with serum samples. The carbon-based DNA framework nano−bio interface would expand the use of SPCE and make electrochemical biosensors more available and valuable in clinical diagnosis.

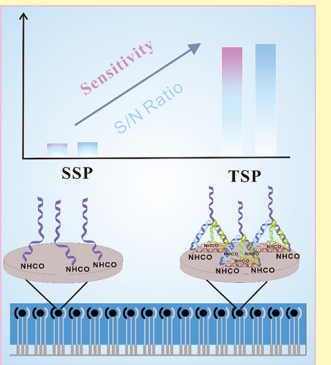

KEYWORDS: *DNA framework, nano−bio interface, high signal-to-noise ratio, screen-printed carbon electrode, electrochemical biosensor*

Downloaded via IMPERIAL COLLEGE LONDON on November 24, 2020 at 11:39:12 (UTC).
See https://pubs.acs.org/sharingguidelines for options on how to legitimately share published articles.

Taking advantages of sensitivity, miniaturization, and low-cost devices, electrochemical biosensors have attracted tremendous interest and hold great promise for practical biosensing use.[1−7] In recent decades, screen printing has become a major branch for the development of electrochemical biosensors because of its possibility of manufacturing massive electrodes in a reproducible, cheap, and disposable format.[8,9] The screen printing carbon electrode (SPCE) can be cheaper and more available than any other kinds of electrodes, such as gold electrodes, for fabricating electrochemical biosensing devices. Also, SPCE permits the feasible incorporation of chemically functionalized materials in a straightforward way[10−12] so that a variety of modifications can be done in the late stage of the functionalization of SPCEs.[13−16] To date, many kinds of SPCEs have been successfully used in proof-of-principle studies to develop prototype biosensors in various configurations for a wide range of analytical applications.[17,18] Nevertheless, several essential technical issues still remain challenging in the development of biosensors with nucleic acid probes on the carbon-based interface. The screen-printed carbon surface is highly rough and has lots of adsorption sites, causing two major problems.[19] First, it is hard to control the orientation of capture probes and the distance between them, which are vital to make them recognize and bind to target molecules including DNA, RNA, and proteins. Second, signaling probes can be easily absorbed onto the carbon surface to produce high background signals. Both low-efficiency capture probes and nonspecifically adsorbed signaling probes would inevitably decrease the sensitivity and signal-to-noise ratio (S/N ratio) of biosensors.

Some inorganic nanomaterial had been used in previous studies to design nanobased interfaces for the improvement of the sensitivity of electrochemical biosensors.[20−24] However, inorganic materials used for carbon-based biosensing interfaces often could not solve the nonspecific adsorption problem and even cause much worse S/N ratio because these modified surfaces often had more complicated structures that lead to more serious adsorption.[6,25−27] Fan's group[28−33] reported that DNA tetrahedron could be successively used in the construction of gold-based electrochemical biosensors. Also, our group had successfully used DNA tetrahedron to develop

Received: August 21, 2020
Accepted: November 4, 2020

© XXXX American Chemical Society

Scheme 1. Schematic Illustration of the DNA Tetrahedron Structure Probe (TSP)-Modified SPCE Electrochemical Platform for Multiplex Biosensing by Simply Changing the Extending Sequences from DNA Tetrahedron

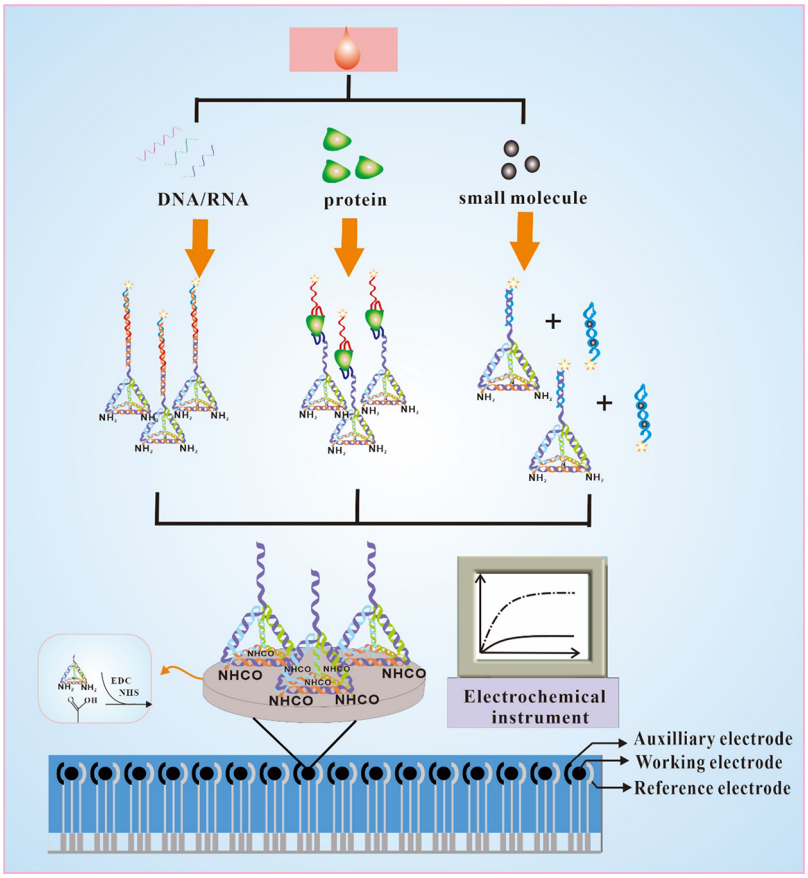

silicon-based biochips.[34] Basic DNA frameworks like tetrahedron are low-cost could be synthesized easily, providing a more feasible and biocompatible choice than inorganic materials. Nevertheless, DNA frameworks used for carbon-based biosensing interfaces have not been investigated until now, even though carbon-based biosensors hold greater promise for practical uses than gold- and silicon-based biosensors.

Herein, we designed a novel carbon-based nano−bio interface for electrochemical biosensors in combination of DNA tetrahedron with SPCE. Each biosensing unit includes a DNA tetrahedron structure decorated with three amine groups and a versatile extended probe DNA. The whole nano−bio structure was synthesized by annealing four well-designed DNA oligonucleotides. The amine-decorated DNA tetrahedron was immobilized on the carbon surface of working electrodes through carboxyl and amino reaction after the SPCE was activated by scanning with cyclic voltammetry. Since the extended DNA probe can be designed to act as different types of recognition and capture probes, various kinds of targets including nucleic acid, protein, and small molecules can be detected (Scheme 1). Importantly, we found that the DNA tetrahedron structure probe (TSP)-decorated SPCE had much higher S/N ratio than that decorated with the single-stranded probe (SSP).

EXPERIMENTAL SECTION

Reagents and Materials. All DNA oligonucleotides (Table S1), GTP, TTP, and CTP were synthesized and purified by Sangon Biotech, while miRNA was purchased from TaKaRa, Inc. (Dalian, PRC). Casein, ATP, Tween 20, thrombin, 1-(3-(dimethylamino)-propyl)-3-ethylcarbodiimidehydrochloride (EDC), *N*-hydroxysulfosuccinimide (NHS), and horseradish peroxidase coupled with avidin (Av-HRP) were purchased from Sigma-Aldrich. 3,3′,5,5′-Tetramethylbenzidine (TMB) substrate was purchased from Neogen. Streptavidin poly-HRP40 Conjugate (SA-polyHRP40) was from Fitzgerald. The washing buffer was phosphate-buffered saline (PBST) solution (10 mM phosphate buffer, 0.14 M NaCl, 2.7 mM KCl, 0.05% (v/v) Tween 20, pH 7.4). Dilution solution for SA-polyHRP40 (10 mM PBS solution at pH 7.4, 1% casein, and 1% BSA). The chemicals mentioned were all used as received, and Milli-Q water (18 MΩ·cm^{-1} resistivity) was used throughout all experiments. MCF-7 cells and PC-3 cells were obtained from Cell Bank of Shanghai Institute of Cell Biology, Chinese Academy of Sciences. Cyclic QIAamp Tissue DNA Mini kit was purchased from Qiagen.

Instruments. Cyclic voltammetry (CV) and amperometry measurements were performed using a portable 16-channel electrochemical workstation. The electrochemical device and SPCE used in this study were homemade, and similar devices and electrode arrays are commercially available from Zhejiang Nanosmart Biotechnology Co., Ltd. (Ningbo, China). The CVs were carried out at a scan rate 100 mV/s from 0 to 0.7 V. Amperometry detection was set at −50 mV, and the electroreduction current was measured at 100 s when the HRP redox reaction was at a steady state. We quantified oligonucleotides using a UV−vis absorption spectrophotometer (Hitachi U-3010, Japan). X-ray photoelectron spectroscopy (XPS) spectra were acquired using an Axis UltraDLD spectrometer (Kratos Analytical, a Shimadzu Group Company) with a monochromatic Al Kα source ($h\nu$ = 1486.6 eV) and a charge neutralization system. The binding energy (BE) scale was internally referenced to the C1s peak (BE for C−C = 284.8 eV). AFM imaging was obtained using a Multimode Nanoscope VIII instrument (Bruker).

https://dx.doi.org/10.1021/acssensors.0c01745
ACS Sens. XXXX, XXX, XXX−XXX

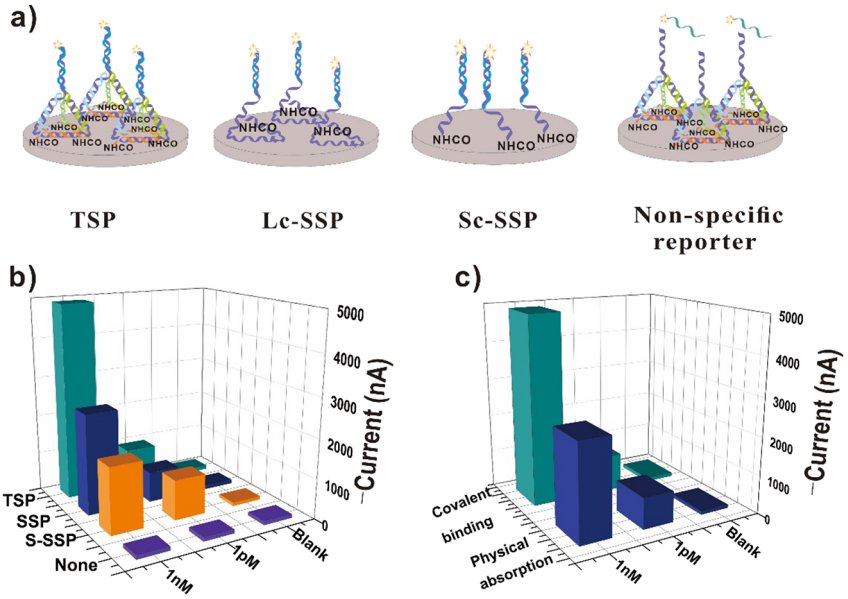

Figure 1. (a) Schematic illustration of probe immobilization for TSP, Lc-SSP, Sc-SSP, and nonspecific reporter DNA on the carbon-based nano–bio interface. (b) DNA hybridization efficiency comparison among TSP, Lc-SSP, and Sc-SSP, (c) Comparison of assembly methods between covalent binding and physical absorption.

Fabrication of the Carbon-Based DNA Framework Nano–Bio Interface. The synthesis of the DNA tetrahedron was the same as the reported papers published by our group.[28,35] The SPCE arrays were pretreated to generate the carboxylic acid groups on the carbon electrode by running CV. We carried out the activation in 10 mM PB (pH 7.0) by CVs at a scan rate of 0.5 V/s, running 100 cycles with a potential from −0.3 to 0.6 V. Ten microliters of freshly prepared 400 mM EDC and 100 mM NHS were dropped to activate carboxylic acid groups for 15 min. Five microliters of DNA tetrahedron solution (1 μM) was dropped followed by 2 h incubation at 37 °C. The same tetrahedron DNA probe without doing the EDC coupling was used as a control (for physical adsorption) by indirectly dropping 5 μL of DNA tetrahedron solution (1 μM) on the carbon electrode. After washing with PBS, the electrode was incubated for 2 h at 25 °C with 50 μL of 1% casein to inactivate binding sites and block nonspecific adsorption sites on the SPCE. The DNA tetrahedron-decorated SPCE arrays were then stored at 4 °C and ready for use. The immobilization of the single strand of DNA was the same as above.

Detection of miRNA. First, the biotinylated signal probe (100 nM) and gap strands (500 nM) were mixed with the target miR-141 in 10 mM PB with 1 M NaCl and 20 mM $MgCl_2$ (pH 7.4) and were incubated in 80 °C for 15 min. The mixture was then kept at 25 °C for more than 20 min. Mixtures (10 uL) were placed on the working electrode and maintained at 37 °C for hybridization. After 2 h incubation, the electrode was washed with 10 mM PBS, then with 3 μL of Av-HRP (0.5 U/mL) or SA-polyHRP40 (1 μg/mL) for 15 min, and was dropped and incubated at 25 °C. Then, the electrodes were measured by the electrochemical workstation. The detection of real miRNA samples was the same as above. The operations were performed in a sterile room. All solutions used in the detection of miRNA were DEPC-treated, and the Eppendorf tubes, microtips, and glass containers were all sterilized to reduce the effect of RNase to avoid the degradation of miRNA.

Detection of Proteins. *Detection of Small Molecules.* A series of ATP samples at variable concentrations were mixed with the antisense signal probe (500 pM) in 20 mM Tris–HCl buffer (pH 7.4) with 100 mM NaCl and 2 mM $MgCl_2$. Then, 10 μL of the mixture was incubated at 37 °C for hybridization. After 1 h incubation, the electrodes were rinsed with 10 mM PBS and incubated with SA-poly-HRP40 (1 μg/mL) for 15 min at room temperature. Then, the electrodes were measured by the electrochemical workstation. The detection of serum samples was the same as above.

RESULTS AND DISCUSSION

Design of the Carbon-Based DNA Framework Nano–Bio Interface. In order to design the carbon-based nano–bio interface, SPCE was first cleaned and activated by CV to produce carboxyl groups on the carbon working electrode. The XPS data revealed that carboxyl groups were generated after activation (Figure S1). The carbon surface was highly rough (Figure S2), which could help immobilize the TSP structure through the high affinity between carboxyl and amine groups. The TSP was self-assembled by annealing one DNA fragment (tetra-A) and three amine-modified DNA fragments (tetra-B, tetra-C, and tetra-D). We characterized the TSP structure by atomic force microscopy (AFM) and polypropylene acyl amine gel electrophoresis (PAGE) (Figure S3). These results proved that the assembly of DNA tetrahedrons was successfully achieved. The assembled TSP contained one extended DNA at one vertex and three amine groups at the other three vertices for its immobilization on the carbon working electrode through amino and carboxyl reaction (Scheme 1). SSP with spacers was designed as controls. We investigated the hybridization performance of the TSP, a long-chain SSP (Lc-SSP, control 1) and a short-chain probe (Sc-SSP, control 2) (Figure 1a). A same reporter DNA modified with biotin in different concentrations was used to directly hybridize with these DNA probes. As can be seen in Figure 1b, the current signal from SPCE functionalized with TSP was significantly higher than that functionalized with both Lc-SSP and Sc-SSP. These could be ascribed to the relative rigid scaffold provided by DNA tetrahedron so that the hybridization fragment of the capture probe could stand upright and keep a free state in the carbon interface. In comparison, capture probes without such a DNA framework were prone to lie down because of the adsorption between the reporter DNA and the carbon surface. Interestingly, SPCE with Lc-SSP produced higher hybridization current signals than that with Sc-SSP. Lc-SSP comprises of a random oligonucleotide sequence (55 bases), which might efficiently keep the hybridization fragment away from the carbon surface in some degree. This result indicated that the

https://dx.doi.org/10.1021/acssensors.0c01745
ACS Sens. XXXX, XXX, XXX−XXX

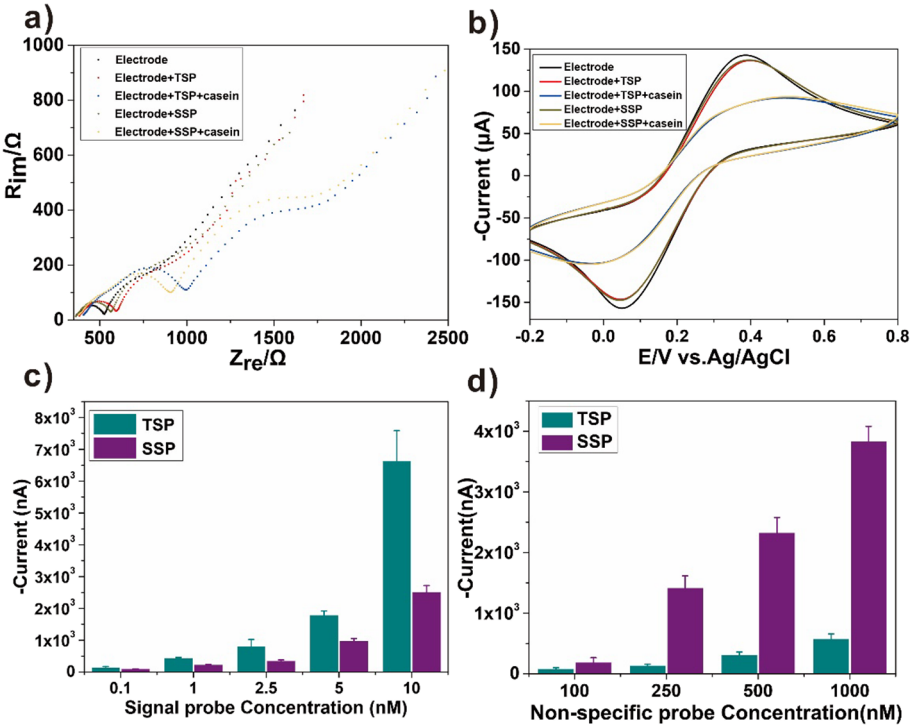

Figure 2. (a) Electrochemical impedance spectroscopy (EIS) and (b) cyclic voltammograms (CVs) of SPCE. Hybridization (c) and adsorption (d) performance of the TSP- and SSP-modified SPCE. The concentration of the modified TSP and SSP was 1 μM; EIS and CV results were obtained in 10 mM, pH 7.4, PBS containing $[Fe(CN)_6]^{3-}/[Fe(CN)_6]^{4-}$ (10 mM, 1:1) and 0.1 M KCl; the impedance frequency range was $10^{-1}-10^{5}$ Hz, and the signal amplitude was 5 mV.

longer random sequence of the probe can adsorb on the carbon surface to avoid the nonspecific adsorption of reporter DNA and help the hybridization sequence to recognize and bind to targets. However, the unordered DNA structure has much lower efficiency than highly ordered DNA tetrahedron. Next, we changed the reporter DNA into the nonspecific biotin-modified DNA and found that the electrochemical signal was as low as the blank one. The result indicates that the adsorption between the short report probe (15 bases) and the carbon interface was very weak. Thus, the electrochemical signal mainly comes from the hybridization between the probe DNA and the reporter DNA rather than the adsorption of nonspecific reporter DNA. Also, we compared the assembly methods of TSP on the carbon surface. As can be seen obviously in Figure 1c, the covalent binding mode between amino and carboxyl got much higher signals and S/N ratio than the physical absorption mode, demonstrating that the former could provide a highly ordered DNA tetrahedron layer for the carbon-based nano−bio interface. This provides us with clear design principles for the design of the probes based on the carbon interface in the following experiments.

Characteristic and Performance Verification of the Carbon-Based DNA Framework Nano−Bio Interface. Electrochemical impedance spectroscopy (EIS) and CV were used to characterize the electron transfer performance of the modified SPCE. As shown in Figure 2a, the Nyquist diagrams of all electrodes consisted of a semicircle at high frequency and a line at low frequency. The diameter of the semicircle reflected the charge transfer resistance. The EIS of the bare SPCE displayed a semicircle with a small diameter at high frequency. After EDC/NHS activation, TSP and SSP were immobilized on the SPCE through the interaction between amine and carboxyl groups, resulting in a slight increase of charge transfer resistance because of the poor conductivity of nucleotide,[36] indicating the successful assembly of TSP and SSP. Casein (1%) as blocking reagents to the electrode was used to inactivate the remaining binding sites and block nonspecific adsorption, leading to a decrease in the electrochemical active surface area of electrodes due to the hindering effect on the electron transfer rate and resulting in the attenuation of redox peaks. Since the carbon interface is highly rough, the DNA tetrahedron could effectively compensate for the surface defects of the carbon interface to reduce nonspecific adsorption of protein and DNA. Further, we used 1% casein as a blocking agent because the molecular weight of casein is small enough to repair smaller defects on the carbon interface that the tetrahedron could not fix up. The CVs in the Figure 2b also proved the successive immobilization of TSP and SSP.

Then, we characterized the hybridization and adsorption performance of TSP- and SSP-functionalized SPCEs. As shown in Figure 2c, the electrochemical signal increased with the concentration of the signaling probe. However, with the same concentration of the signaling probe, the TSP-modified SPCE exhibited much higher signal intensity than the SSP-modified SPCE, showing a much better hybridization performance. In the comparison of absorption performance, we adopted a random sequence of DNA to react with the immobilized probe on the SPCE, and the TSP-modified SPCE obviously showed a weak adsorption interaction than the SSP-modified SPCE at the same nonspecific DNA concentration (Figure 2d). Therefore, the TSP-functionalized carbon interface showed higher hybridization and lower adsorption performance than the SSP-functionalized one, which could absolutely improve the S/N ratio in the nucleic acid reaction and show huge potential for practical biosensing uses. The repeatability is also

https://dx.doi.org/10.1021/acssensors.0c01745
ACS Sens. XXXX, XXX, XXX−XXX

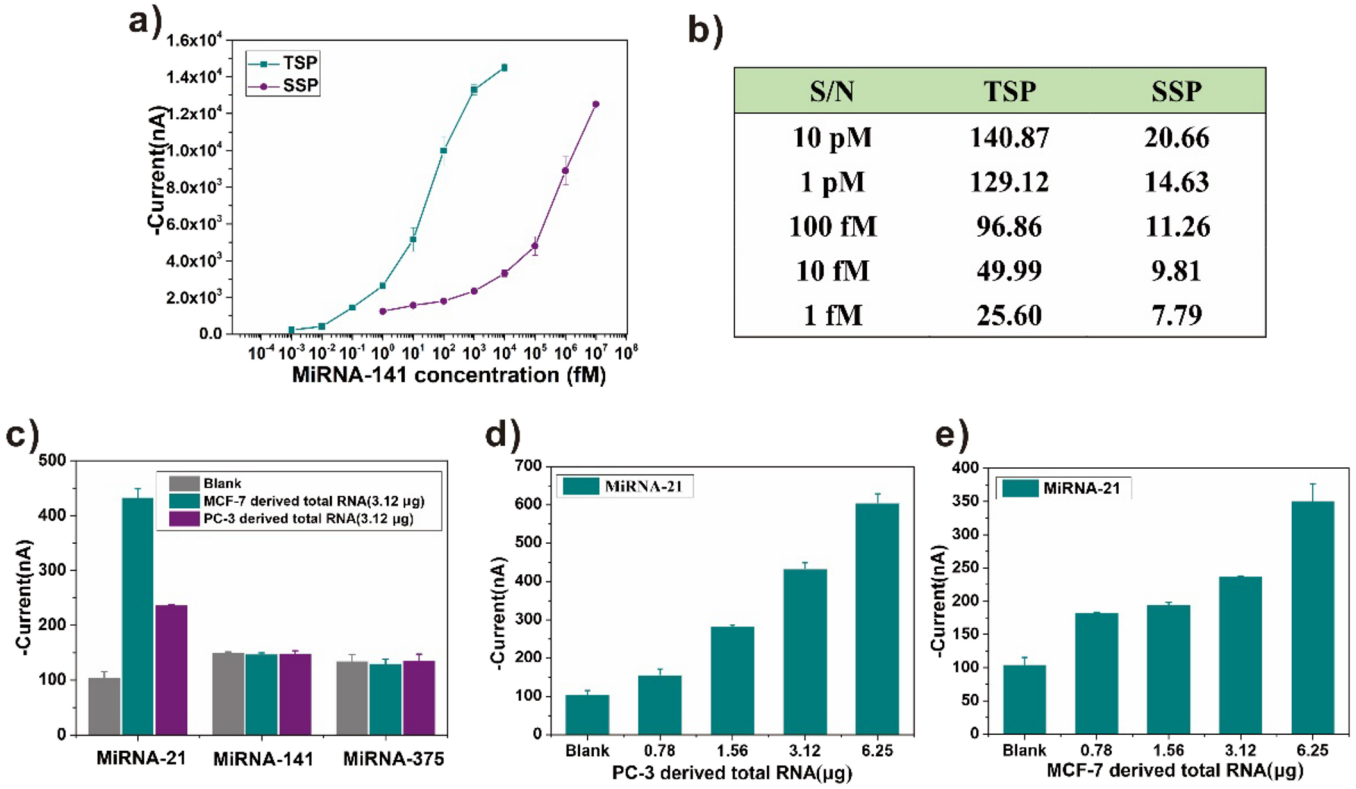

S/N	TSP	SSP
10 pM	140.87	20.66
1 pM	129.12	14.63
100 fM	96.86	11.26
10 fM	49.99	9.81
1 fM	25.60	7.79

Figure 3. (a) Logarithmic plot of amperometry current versus miRNA-141 concentration for TSP- and SSP-modified carbon-based electrochemical biosensors. The dynamic range is broad and spans from 10 aM to 10 pM. (b) Comparison of S/N ratio in the detection of different concentration of miRNA-141 with TSP- and SSP-modified carbon-based nano−bio interface. (c) Detection of three kinds of miRNAs with the TSP-modified carbon-based electrochemical biosensor. (d,e) Detection of different quantities of miRNA-21 in PC-3 and MCF-7 cells with the TSP-modified carbon-based electrochemical biosensor.

an important performance indicator in the construction of biosensors. In order to test the repeatability of our DNA tetrahedron-based carbon interface, the electrochemical responses to the 10 nM signal probe were repeatedly measured over a period (five days). As can be seen in Figure S4, the average response of the current signal produced a fluctuation of no more than 10%. Therefore, our DNA tetrahedron-based carbon interface shows a high repeatability in the construction of biosensors.

Universal Biosensing Strategy Based on the DNA Framework Nano−Bio Interface. Having demonstrated the DNA framework nano−bio interface with improved biorecognition capacity and weak adsorption performance, we developed a universal TSP-functionalized carbon-based biosensing platform to achieve the multiplex detection of various kinds of bioactive analytics including proteins, miRNAs, and small molecules (Scheme 1). MicroRNA-141 (miRNA-141, a promising cancer biomarker), thrombin (crucial in physiological and pathological coagulation), and ATP (to participate in the cellular energy transfer) were chosen as model target molecules. We have designed a specific detection strategy for each analyte to get the greatest assay performance by simply changing the sequence extending from DNA tetrahedron. The 16-channel homemade electrochemical biosensing device equipped with 16-channel SPCE arrays was used for multiplex and high-throughput detection.

Detection of miRNA. MiRNAs have been associated with the development of cancer and could be applied as potential biomarkers for the early diagnosis of cancer.[37,38] Here, a gap hybridization strategy was designed for miRNA-141 biosensing detection.[39] At first, some important biosensing parameters had been optimized, including reaction temperature and the concentration of the biotin-signaling probe (see Figure S5). We found that a higher S/N ratio could be obtained when the reaction temperature was 37 °C and the concentration of the biotin-signal probe was 100 nM. As shown in Figure 3a, as the miRNA-141 concentration increased from 10 aM to 10 pM, the electrochemical signal intensity increased gradually. Of note, TSP-functionalized carbon-based electrochemical biosensor for miRNA-141 had a broad dynamic range (five decades) with higher S/N ratio (Figure 3b) and aM level limit of detection (LOD, we determine the LOD as the lowest detected concentration whose signal was higher than the blank control signal plus three standard deviations). 10 aM of LOD for miRNA-141 means that 60 miRNA-141 molecules could be detected in 10 μL samples. The super-high sensitivity was ascribed to the consistently favorable orientation of DNA tetrahedron on the carbon-based nano−bio interface, which could avoid possible steric crowding and electrostatic interaction and the adsorption of the nonspecific DNA and protein. As a control, we also used the SSP-modified SPCE to detect miRNA-141 in the same concentration range, showing three orders of magnitude smaller LOD (10 fM) than the TSP-functionalized carbon interface. Then, we tried to examine the suitability of TSP-functionalized carbon interface for complex sample system by using total RNAs extracted from the MCF-7 and the PC-3 cell lines. Different target miRNAs were detected by changing the sequence of helper DNA without changing the sequence of capture DNA and the signaling probe DNA. As shown in Figure 3c, miRNA-21 could be detected in the total

https://dx.doi.org/10.1021/acssensors.0c01745
ACS Sens. XXXX, XXX, XXX−XXX

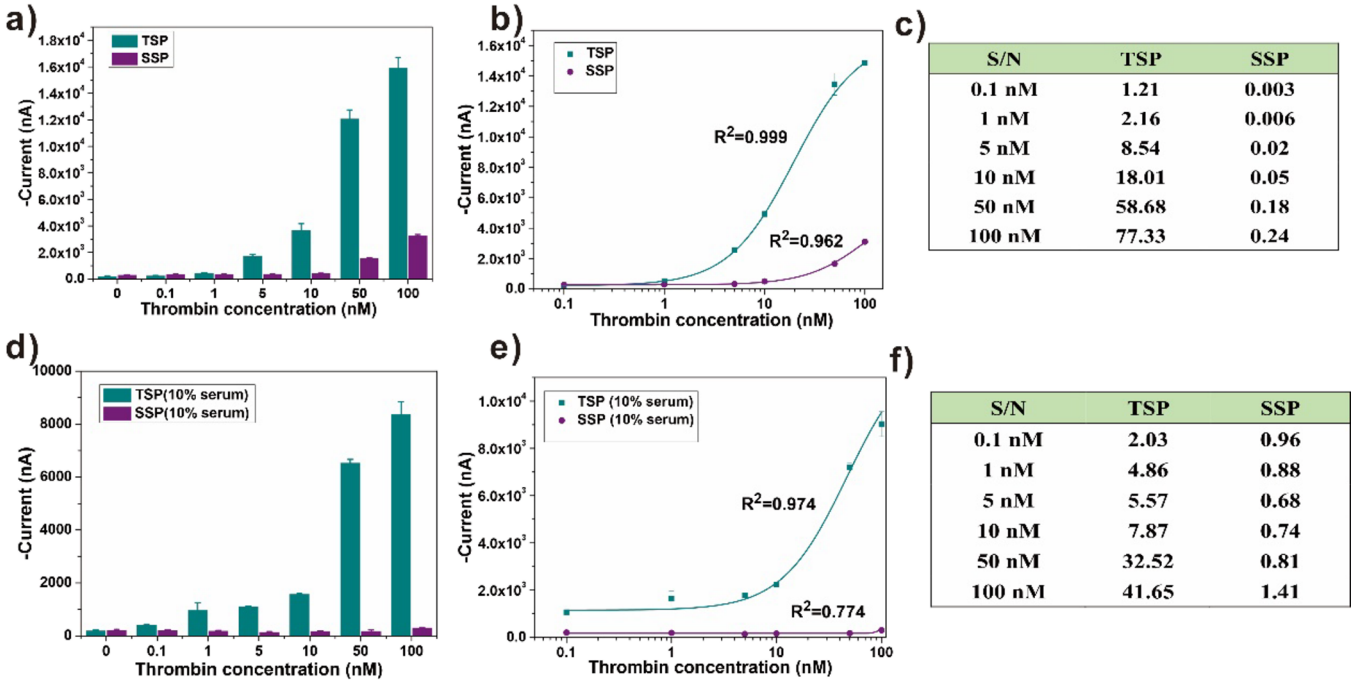

S/N	TSP	SSP
0.1 nM	1.21	0.003
1 nM	2.16	0.006
5 nM	8.54	0.02
10 nM	18.01	0.05
50 nM	58.68	0.18
100 nM	77.33	0.24

S/N	TSP	SSP
0.1 nM	2.03	0.96
1 nM	4.86	0.88
5 nM	5.57	0.68
10 nM	7.87	0.74
50 nM	32.52	0.81
100 nM	41.65	1.41

Figure 4. Concentration profile for the detection of thrombin in buffer (a) and 10% serum (d) with TSP- and SSP-modified carbon-based electrochemical biosensor. The comparison of S/N ratio in the detection of different concentration of thrombin in buffer (c) and 10% serum (f) with TSP- and SSP-modified carbon-based nano−bio interface. Logarithmic plot of amperometry current vs thrombin concentration in buffer (b) and 10% serum (e) for the TSP- and SSP-modified carbon-based electrochemical biosensor.

miRNAs from the MCF-7 and PC-3 cell lines, while the electrochemical signals of miRNA-141 and miRNA-375 were as same as the blank control, indicating that the quantity of miRNA-141 and miRNA-375 was lower in MCF-7 and PC-3 cells. The results were consistent with the reported content of miRNA-21 in MCF-7 and PC-3 cells in the previous studies.[40−43] Also, we investigated the required amount of extracted total miRNA in the cell lines and found that as little as 0.78 μg miRNA was enough for the detection of miRNA-21 in MCF-7 and PC-3 cell lines (Figure 3d,e). Therefore, the designed carbon-based nano−bio interface could be applied to detect multiple miRNAs in tissue samples.

Detection of Proteins. We challenged the TSP-modified carbon-based electrochemical biosensor for the detection of proteins. Generally, SPCE was used for the establishment of the electrochemical immunosensor.[44−46] The rough carbon surface could help the immobilization of antibodies. However, the orientation direction and the density of antibodies would limit their recognition activity and reduce the sensitivity of protein detection. Here, we took the thrombin for example and designed a double-aptamer sandwich strategy for the detection of the protein. The 15-base thrombin aptamer was involved in the intending sequence of the DNA tetrahedron, while another 29-base thrombin aptamer was decorated with the biotin to act as a reporting probe. Detailed information for the optimization of important parameters can be found in the Supporting Information, Figure S6. Especially, the dilution and reaction buffers were 1% BSA. Within 30 min of reaction, higher positive signals could be obtained.

The results for thrombin assay could be seen in Figure 4a. We challenged the TSP- and SSP-modified carbon-based electrochemical biosensor with a series of diluted samples (100 pM to 100 nM thrombin). The electrochemical signal from the TSP-modified SPCEs was much higher than that from the SSP-modified ones, 0.1 nM thrombin could be detected by the TSP-modified SPCE, while 10 nM thrombin could be detected by the SSP-modified SPCE. Also, we challenged its feasibility and capability in the detection of thrombin in 10% human serum (Figure 4d,e). The TSP-modified SPCE could work well with 10% serum, while the SSP-modified one showed only weak correlation with different concentrations of thrombin. The S/N ratio by using the TSP-modified SPCE was much higher than the detection with SSP-modified SPCE not only in the buffer but also in the 10% serum (Figure 4c,f). These results demonstrated that the TSP-functionalized carbon biosensing interface could facilitate the folding of aptamer against target proteins and showed much better detection performance.

Detection of Small Molecules. ATP was used as a mode molecule to investigate the TSP-modified carbon-based electrochemical biosensor for the detection of small molecules. ATP is a source of intracellular energy and participates in a series of biological processes.[47] Here, we designed a competitive strategy that an aptamer could either participate in recognizing ATP or in hybridization with the extending strand from the tetrahedron (Scheme 1). In the absence of ATP, the aptamer participated in hybridization with the capture probe, and the higher electrochemical signal could be achieved. With the increase of the concentration of ATP, the less biotin-decorated aptamer would participate in the hybridization, resulting in the decease of current signals ("signal off" mode; I_{max} and I were defined as the electrochemical signal without and with ATP, respectively). Some important parameters had been optimized (see more details in the Supporting Information, Figure S7). Especially, 37 °C for reaction temperature, 45 min for reaction procedure, and 500 nM for the concentration of biotin-decorated aptamer report probes were chosen so that higher current signal change could

https://dx.doi.org/10.1021/acssensors.0c01745
ACS Sens. XXXX, XXX, XXX−XXX

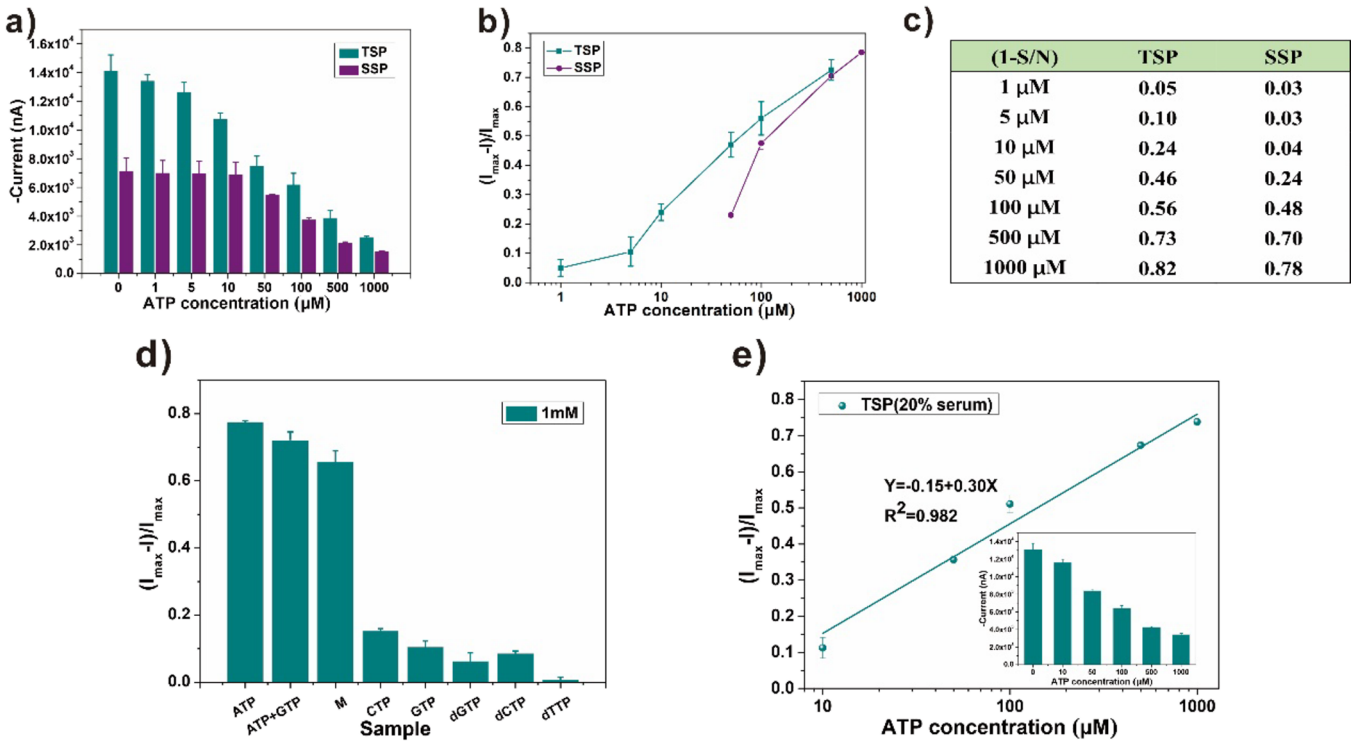

Figure 5. (a) Concentration profile for detection of ATP in buffer with TSP- and SSP-modified carbon-based electrochemical biosensor. (b) Logarithmic plot of $(I_{max} - I)/I$ versus ATP concentration with TSP- and SSP-modified carbon-based electrochemical biosensor. Electrochemical signal without ATP as I_{max} and the electrochemical signal with the ATP as I. (c) Comparison of S/N ratio in the detection of different concentrations of ATP with TSP- and SSP-modified carbon-based nano−bio interface. (d) Selectivity investigation of TSP-modified carbon-based electrochemical biosensor for the detection of ATP (1 mM) against other control analogue molecules and the mixture of these analogues (GTP, TTP, CTP, dGTP, dCTP, and dTTP). (e) $(I_{max} - I)/I$ versus ATP concentration in 20% serum with TSP-modified carbon-based electrochemical biosensor.

be obtained. The TSP-modified SPCE showed obviously higher current signal change than the SSP-modified one (Figure 5a). Since the designed biosensing configuration for ATP is "signal off" mode, which is different from the detection of miRNA and protein, we use the ratio of signal change (I_{max} − I) and background signal (I_{max}) to characterize the sensitivity of ATP detection (Figure 5b). ATP (1 μM) could be detected by the TSP- modified SPCE, while only 50 μM ATP could be detected by the SSP-modified one. The $(I_{max} - I)/I_{max}$, that is to say (1 − S/N) ratio from the TSP-functionalized carbon interface was higher than that from the SSP-functionalized one (Figure 5c). The specificity of the TSP-modified carbon-based electrochemical biosensor for the detection of ATP was investigated by incubating ATP with its analogues such as cytidine triphosphate (CTP), guanosine triphosphate (GTP), uridine triphosphate (UTP), and their mixture. We found that the changes of electrochemical signals resulted from CTP, GTP, UTP, and the mixture were less than 20% of that of ATP, even if their concentrations were the same as ATP (Figure 5d). These results suggested that the proposed biosensor had excellent selectivity for ATP. Also, the biosensor was used to detect ATP in 20% human serum samples. The current signals increased proportionally as concentration of ATP increased (from 10 μM to 1 mM; log-linear fitting equation: $y = 0.3x - 0.15$; R^2: 0.982). We could detect as low as 10 μM ATP (Figure 5e). The results demonstrated that the TSP-modified carbon-based electrochemical biosensor can be available for quantification of small molecules in real-life samples.

Advantages of the TSP-Functionalized Carbon-Based Nano−Bio Interface. The TSP-functionalized carbon-based nano−bio interface has solved two problems in the application of SPCE for the detection based on nucleic acid probes. One problem is that the rough surface of SPCE could adsorb DNA probes randomly to hinder DNA hybridization, and the other problem is that the carbon-based surface could cause nonspecific adsorption to increase the background signal. Here, the TSP-functionalized carbon-based nano−bio interface could provide a rigid foothold to improve the hybridization and binding performance and reduce the background adsorption, greatly improving the S/N ratio. Especially, we adopted the multiplex SPCE array other than the conventional electrode to gain extra advantages (see Table S2). Therefore, the combination of DNA framework and SPCE has significantly expanded the practical application of SPCE for clinical diagnostics in the future. Nevertheless, there are still much work to do for the use of DNA nanostructures in the improvement of the carbon-based interface, including the different structures and sizes of the DNA tetrahedron and the assembly density of the DNA nanostructure. Thus, much more efforts are still required to explore the role of DNA nanostructures played in carbon-based interfaces.

CONCLUSIONS

In summary, we have established a novel platform for the construction of carbon-based biosensing interface by bonding rationally well-designed TSP onto SPCE with covalent coupling. Also, a multiplex and universal platform has been

https://dx.doi.org/10.1021/acssensors.0c01745
ACS Sens. XXXX, XXX, XXX−XXX

developed for the highly sensitive and selective detection of various kinds of bioactive molecules including proteins, miRNAs, and small molecules. The TSP-functionalized SPCE showed obvious higher S/N ratio in comparison with the SSP-functionalized one. The disposable functionalized SPCE has advantages of low-cost, easy-making, good stability, and reproducibility, holding great promise in the practical clinical diagnosis. It is worth noting that the TSP-functionalized carbon-based biosensor can easily be integrated with microfluidic devices to provide an all-in-one solution for the rapid analysis of real-life samples. Especially, in combination with portable electrochemical devices and smartphones, it would have the potential to achieve point-of-care testing (POCT) in the future.

■ ASSOCIATED CONTENT

Supporting Information

The Supporting Information is available free of charge at https://pubs.acs.org/doi/10.1021/acssensors.0c01745.

XPS and SEM of the carbon electrode; AFM and PAGE image of the DNA tetrahedron; repeatability of the DNA tetrahedron-based biosensor; optimal conditions in the detection of miRNA-141, thrombin, and ATP TSP-modified carbon-based nano−bio electrochemical sensor; DNA and microRNA sequences employed in this work; and comparison of the properties of the conventional electrode with SPCE (PDF)

■ AUTHOR INFORMATION

Corresponding Authors

Xianting Ding − *State Key Laboratory of Oncogenes and Related Genes, Institute for Personalized Medicine, School of Biomedical Engineering, Shanghai Jiao Tong University, Shanghai 200030, China;* orcid.org/0000-0002-1549-3499; Email: dingxianting@sjtu.edu.cn

Shiping Song − *Shanghai Synchrotron Radiation Facility, Zhangjiang Lab, Shanghai Advanced Research Institute, Chinese Academy of Sciences, Shanghai 201210, China; Shanghai Institute of Applied Physics, Chinse Academy of Sciences, Shanghai 201800, China;* orcid.org/0000-0002-0791-8012; Email: songshiping@sinap.ac.cn

Authors

Jing Su − *Shanghai Synchrotron Radiation Facility, Zhangjiang Lab, Shanghai Advanced Research Institute, Chinese Academy of Sciences, Shanghai 201210, China; State Key Laboratory of Oncogenes and Related Genes, Institute for Personalized Medicine, School of Biomedical Engineering, Shanghai Jiao Tong University, Shanghai 200030, China*

Wenhan Liu − *Shanghai Institute of Applied Physics, Chinse Academy of Sciences, Shanghai 201800, China; University of Chinese Academy of Sciences, Beijing 100049, China*

Shixing Chen − *Shanghai Institute of Applied Physics, Chinse Academy of Sciences, Shanghai 201800, China*

Wangping Deng − *Shanghai Institute of Applied Physics, Chinse Academy of Sciences, Shanghai 201800, China*

Yanzhi Dou − *Shanghai Institute of Applied Physics, Chinse Academy of Sciences, Shanghai 201800, China; University of Chinese Academy of Sciences, Beijing 100049, China*

Zhihan Zhao − *Shanghai Institute of Applied Physics, Chinse Academy of Sciences, Shanghai 201800, China*

Jianyong Li − *Shanghai Institute of Applied Physics, Chinse Academy of Sciences, Shanghai 201800, China; University of Chinese Academy of Sciences, Beijing 100049, China*

Zhenhua Li − *Shanghai Institute of Applied Physics, Chinse Academy of Sciences, Shanghai 201800, China; University of Chinese Academy of Sciences, Beijing 100049, China*

Heng Yin − *Department of Spine, TCM Hospital Affiliated to Nanjing University of Chinese Medicine, Wuxi 214071, China*

Complete contact information is available at: https://pubs.acs.org/10.1021/acssensors.0c01745

Author Contributions

#J.S. and W.L. contributed equally to this work. The manuscript was written through contributions of all authors. All authors have given approval to the final version of the manuscript.

Notes

The authors declare no competing financial interest.

■ ACKNOWLEDGMENTS

This work was supported by the National Research Programs from Ministry of Science and Technology of China (2018YFF0212803) and the National Natural Science foundation of China (21974147, 81973878, 81871448, and 32000921).

■ REFERENCES

(1) Wang, J. Electrochemical biosensors: towards point-of-care cancer diagnostics. *Biosens. Bioelectron.* **2006**, *21*, 1887−1892.

(2) Wang, J. Portable electrochemical systems. *TrAC, Trends Anal. Chem.* **2002**, *21*, 226−232.

(3) Ronkainen, N. J.; Halsall, H. B.; Heineman, W. R. Electrochemical biosensors. *Chem. Soc. Rev.* **2010**, *39*, 1747−1763.

(4) Hanrahan, G.; Patil, D. G.; Wang, J. Electrochemical sensors for environmental monitoring: design, development and applications. *J. Environ. Monit.* **2004**, *6*, 657−664.

(5) Xu, X.; Zhang, S.; Chen, H.; Kong, J. Integration of electrochemistry in micro-total analysis systems for biochemical assays: recent developments. *Talanta* **2009**, *80*, 8−18.

(6) Bandodkar, A. J.; Wang, J. Non-invasive wearable electrochemical sensors: a review. *Trends Biotechnol.* **2014**, *32*, 363−371.

(7) Winther-Jensen, B.; Krebs, F. C. High-conductivity large-area semi-transparent electrodes for polymer photovoltaics by silk screen printing and vapour-phase deposition. *Sol. Energy Mater. Sol. Cells* **2006**, *90*, 123−132.

(8) Dequaire, M.; Heller, A. Screen printing of nucleic acid detecting carbon electrodes. *Anal. Chem.* **2002**, *74*, 4370−4377.

(9) Krebs, F. C.; Jørgensen, M.; Norrman, K.; Hagemann, O.; Alstrup, J.; Nielsen, T. D.; Fyenbo, J.; Larsen, K.; Kristensen, J. A complete process for production of flexible large area polymer solar cells entirely using screen printing—first public demonstration. *Sol. Energy Mater. Sol. Cells* **2009**, *93*, 422−441.

(10) Wang, J.; Tian, B.; Nascimento, V. B.; Angnes, L. Performance of screen-printed carbon electrodes fabricated from different carbon inks. *Electrochim. Acta* **1998**, *43*, 3459−3465.

(11) Fanjul-Bolado, P.; Hernández-Santos, D.; Lamas-Ardisana, P. J.; Martín-Pernía, A.; Costa-García, A. Electrochemical characterization of screen-printed and conventional carbon paste electrodes. *Electrochim. Acta* **2008**, *53*, 3635−3642.

(12) Wang, J.; Pedrero, M.; Sakslund, H.; Hammerich, O.; Pingarron, J. Electrochemical activation of screen-printed carbon strips. *Analyst* **1996**, *121*, 345−350.

(13) Tangkuaram, T.; Ponchio, C.; Kangkasomboon, T.; Katikawong, P.; Veerasai, W. Design and development of a highly

stable hydrogen peroxide biosensor on screen printed carbon electrode based on horseradish peroxidase bound with gold nanoparticles in the matrix of chitosan. *Biosens. Bioelectron.* **2007**, *22*, 2071−2078.
(14) Chikae, M.; Idegami, K.; Kerman, K.; Nagatani, N.; Ishikawa, M.; Takamura, Y.; Tamiya, E. Direct fabrication of catalytic metal nanoparticles onto the surface of a screen-printed carbon electrode. *Electrochem. Commun.* **2006**, *8*, 1375−1380.
(15) Lin, Y.; Lu, F.; Wang, J. Disposable carbon nanotube modified screen−printed biosensor for amperometric detection of organophosphorus pesticides and nerve agents. *Electroanalysis* **2004**, *16*, 145−149.
(16) Suprun, E.; Evtugyn, G.; Budnikov, H.; Ricci, F.; Moscone, D.; Palleschi, G. Acetylcholinesterase sensor based on screen-printed carbon electrode modified with prussian blue. *Anal. Bioanal. Chem.* **2005**, *383*, 597−604.
(17) Tudorache, M.; Bala, C. Biosensors based on screen-printing technology, and their applications in environmental and food analysis. *Anal. Bioanal. Chem.* **2007**, *388*, 565−578.
(18) Huang, S.-H.; Liao, H.-H.; Chen, D.-H. Simultaneous determination of norepinephrine, uric acid, and ascorbic acid at a screen printed carbon electrode modified with polyacrylic acid-coated multi-wall carbon nanotubes. *Biosens. Bioelectron.* **2010**, *25*, 2351−2355.
(19) Min, K.; Yoo, Y. J. Amperometric detection of dopamine based on tyrosinase−SWNTs−Ppy composite electrode. *Talanta* **2009**, *80*, 1007−1011.
(20) Karadeniz, H.; Erdem, A.; Caliskan, A. Electrochemical monitoring of DNA hybridization by multiwalled carbon nanotube based screen printed electrodes. *Electroanalysis* **2008**, *20*, 1932−1938.
(21) Ping, J.; Wu, J.; Wang, Y.; Ying, Y. Simultaneous determination of ascorbic acid, dopamine and uric acid using high-performance screen-printed graphene electrode. *Biosens. Bioelectron.* **2012**, *34*, 70−76.
(22) Kerman, K.; Saito, M.; Tamiya, E.; Yamamura, S.; Takamura, Y. Nanomaterial-based electrochemical biosensors for medical applications. *TrAC, Trends Anal. Chem.* **2008**, *27*, 585−592.
(23) Wang, J. Nanomaterial-based electrochemical biosensors. *Analyst* **2005**, *130*, 421−426.
(24) Wang, J. Carbon−nanotube based electrochemical biosensors: A review. *Electroanalysis* **2005**, *17*, 7−14.
(25) Guo, Z.; Xu, X.-F.; Li, J.; Liu, Y.-W.; Zhang, J.; Yang, C. Ordered mesoporous carbon as electrode modification material for selective and sensitive electrochemical sensing of melamine. *Sens. Actuators, B* **2014**, *200*, 101−108.
(26) López-Naranjo, E. J.; González-Ortiz, L. J.; Apátiga, L. M.; Rivera-Muñoz, E. M.; Manzano-Ramírez, A. Transparent Electrodes: A Review of the Use of Carbon-Based Nanomaterials. *J. Nanomater.* **2016**, 1.
(27) Cheng, Y.; Hao, Z.; Hao, C.; Deng, Y.; Li, X.; Li, K.; Zhao, Y. A review of modification of carbon electrode material in capacitive deionization. *RSC Adv.* **2019**, *9*, 24401−24419.
(28) Pei, H.; Lu, N.; Wen, Y.; Song, S.; Liu, Y.; Yan, H.; Fan, C. A DNA Nanostructure-based Biomolecular Probe Carrier Platform for Electrochemical Biosensing. *Adv. Mater.* **2010**, *22*, 4754−4758.
(29) Ge, Z.; Lin, M.; Wang, P.; Pei, H.; Yan, J.; Shi, J.; Huang, Q.; He, D.; Fan, C.; Zuo, X. Hybridization chain reaction amplification of microRNA detection with a tetrahedral DNA nanostructure-based electrochemical biosensor. *Anal. Chem.* **2014**, *86*, 2124−2130.
(30) Wen, Y.; Pei, H.; Wan, Y.; Su, Y.; Huang, Q.; Song, S.; Fan, C. DNA nanostructure-decorated surfaces for enhanced aptamer-target binding and electrochemical cocaine sensors. *Anal. Chem.* **2011**, *83*, 7418−7423.
(31) Lin, M.; Wen, Y.; Li, L.; Pei, H.; Liu, G.; Song, H.; Zuo, X.; Fan, C.; Huang, Q. Target-responsive, DNA nanostructure-based E-DNA sensor for microRNA analysis. *Anal. Chem.* **2014**, *86*, 2285−2288.
(32) Chen, X.; Zhou, G.; Song, P.; Wang, J.; Gao, J.; Lu, J.; Fan, C.; Zuo, X. Ultrasensitive electrochemical detection of prostate-specific antigen by using antibodies anchored on a DNA nanostructural scaffold. *Anal. Chem.* **2014**, *86*, 7337−7342.
(33) Zhou, G.; Lin, M.; Song, P.; Chen, X.; Chao, J.; Wang, L.; Huang, Q.; Huang, W.; Fan, C.; Zuo, X. Multivalent capture and detection of cancer cells with DNA nanostructured biosensors and multibranched hybridization chain reaction amplification. *Anal. Chem.* **2014**, *86*, 7843−7848.
(34) Li, Z.; Zhao, B.; Wang, D.; Wen, Y.; Liu, G.; Dong, H.; Song, S.; Fan, C. DNA nanostructure-based universal microarray platform for high-efficiency multiplex bioanalysis in biofluids. *ACS Appl. Mater. Interfaces* **2014**, *6*, 17944−17953.
(35) Lin, M.; Song, P.; Zhou, G.; Zuo, X.; Aldalbahi, A.; Lou, X.; Shi, J.; Fan, C. Electrochemical detection of nucleic acids, proteins, small molecules and cells using a DNA-nanostructure-based universal biosensing platform. *Nat. Protoc.* **2016**, 1244.
(36) Kasumov, A. Y.; Klinov, D. V.; Roche, P. E.; Guéron, S.; Bouchiat, H. Thickness and low-temperature conductivity of DNA molecules. *Appl. Phys. Lett.* **2004**, *84*, 1007−1009.
(37) Chin, L. J.; Slack, F. J. A truth serum for cancer–microRNAs have major potential as cancer biomarkers. *Cell Res.* **2008**, *18*, 983.
(38) Mitchell, P. S.; Parkin, R. K.; Kroh, E. M.; Fritz, B. R.; Wyman, S. K.; Pogosova-Agadjanyan, E. L.; Peterson, A.; Noteboom, J.; O'Briant, K. C.; Allen, A.; Lin, D. W.; Urban, N.; Drescher, C. W.; Knudsen, B. S.; Stirewalt, D. L.; Gentleman, R.; Vessella, R. L.; Nelson, P. S.; Martin, D. B.; Tewari, M. Circulating microRNAs as stable blood-based markers for cancer detection. *Proc. Natl. Acad. Sci. U. S. A.* **2008**, *105*, 10513−10518.
(39) Wen, Y.; Li, L.; Li, J.; Lin, M.; Liu, G.; Liang, W.; Xu, L.; Li, Y.; Zuo, X.; Ren, S.; Zhu, Y. DNA Framework-Mediated Electrochemical Biosensing Platform for Amplification-Free MicroRNA Analysis. *Anal. Chem.* **2020**, *92*, 4498−4503.
(40) Yan, L.-X.; Huang, X.-F.; Shao, Q.; Huang, M.-Y.; Deng, L.; Wu, Q.-L.; Zeng, Y.-X.; Shao, J.-Y. MicroRNA miR-21 overexpression in human breast cancer is associated with advanced clinical stage, lymph node metastasis and patient poor prognosis. *RNA* **2008**, *14*, 2348−2360.
(41) Kachakova, D.; Mitkova, A.; Popov, E.; Popov, I.; Vlahova, A.; Dikov, T.; Christova, S.; Mitev, V.; Slavov, C.; Kaneva, R. Combinations of serum prostate-specific antigen and plasma expression levels of let-7c, miR-30c, miR-141, and miR-375 as potential better diagnostic biomarkers for prostate cancer. *DNA Cell Biol.* **2015**, *34*, 189−200.
(42) Yan, J.-W.; Lin, J.-S.; He, X.-X. The emerging role of miR-375 in cancer. *Int. J. Cancer* **2014**, *135*, 1011−1018.
(43) Yaman Agaoglu, F.; Kovancilar, M.; Dizdar, Y.; Darendeliler, E.; Holdenrieder, S.; Dalay, N.; Gezer, U. Investigation of miR-21, miR-141, and miR-221 in blood circulation of patients with prostate cancer. *Tumor Biol.* **2011**, *32*, 583−588.
(44) Deng, W.; Xu, B.; Hu, H.; Li, J.; Hu, W.; Song, S.; Feng, Z.; Fan, C. Diagnosis of schistosomiasis japonica with interfacial co-assembly-based multi-channel electrochemical immunosensor arrays. *Sci. Rep.* **2013**, *3*, 1789.
(45) Dou, Y.; Jiang, Z.; Deng, W.; Su, J.; Chen, S.; Song, H.; Aldalbahi, A.; Zuo, X.; Song, S.; Shi, J.; Fan, C. Portable detection of clenbuterol using a smartphone-based electrochemical biosensor with electric field-driven acceleration. *Electroanal. Chem.* **2016**, *781*, 339−344.
(46) Wan, Y.; Deng, W.; Su, Y.; Zhu, X.; Peng, C.; Hu, H.; Peng, H.; Song, S.; Fan, C. Carbon nanotube-based ultrasensitive multiplexing electrochemical immunosensor for cancer biomarkers. *Biosens. Bioelectron.* **2011**, *30*, 93−99.
(47) Nemoto, I.; Ogura, K.; Toyotama, H. Estimation of the energy of cytoplasmic movements by magnetometry: Effects of temperature and intracellular concentration of ATP. *IEEE T Bio-Med Eng* **1989**, *36*, 598−607.

https://dx.doi.org/10.1021/acssensors.0c01745
ACS Sens. XXXX, XXX, XXX−XXX